Journal of Alloys and Compounds 506 (2010) 496–499

Contents lists available at ScienceDirect

Journal of Alloys and Compounds

journal homepage: www.elsevier.com/locate/jallcom

Time-resolved photoluminescence study of stabilised iron–porous silicon nanocomposites

M. Rahmani [a], H. Ajlani [a], A. Moadhen [a], M.-A. Zaïbi [a,b,*], L. Haji [c], M. Oueslati [a]

[a] Unité de Spectroscopie Raman, Faculté des Sciences de Tunis, Université Tunis El Manar, 2092 ElManar, Tunis, Tunisia
[b] Ecole Supérieure des Sciences et Techniques de Tunis Université de Tunis, 5 Av. Taha Hussein, 1008 Montfleury, Tunis, Tunisia
[c] Université Européenne de Bretagne, CNRS FOTON-UMR 6082, 6 rue de Kérampont, B.P. 80518, 22305 Lannion Cedex, France

ARTICLE INFO

Article history:
Received 14 April 2010
Received in revised form 7 July 2010
Accepted 7 July 2010
Available online 15 July 2010

Keywords:
Porous silicon
Iron
Time-resolved photoluminescence
Decay time

ABSTRACT

Porous silicon (PS) passivated by iron (PS/Fe) shows an intense, board and stable photoluminescence (PL) band centred at 1.77 eV. The time-resolved photoluminescence (TRPL) of PS and PS/Fe, in the range of some tenth of μs, were investigated at room temperature. Contrary to PS, the TRPL spectrum of PS/Fe exhibits a multi-band profile, attributed to the presence of iron in porous silicon matrix. Hence, the passivation of PS by iron provides the formation of two states located in the PS band gap. The PL decay line shape, in PS and PS/Fe, is well described by stretched exponential. The decay time (τ) in PS has been found lower than that of PS/Fe which is due to the reduction of the non-radiative transitions. Such paths occur when excited carriers escape by tunnelling from less passivated nanocrystallites silicon. The analyses of the TRPL spectra as well as the decay times approve the passivation of Si nanocrystallites by iron.

1. Introduction

Following the observation of visible photoluminescence (PL) in porous silicon (PS) [1], several studies were motivated by fundamental research as well as by technological applications. Light-emitting Si devices could eventually result in a new generation of Si chips and consequently extend the functionality of Si technology from microelectronics into optoelectronics.

The PL time dependence of PS was important because it shed light on the importance of the luminescence mechanism (radiative process following pulsed-excitation) and determined the range of technological applications based on such a luminescent material. Nevertheless, time-resolved photoluminescence spectroscopy (TRPL) of PS has been extensively studied [2–5] and some workers have reported that at room temperature the PL decay time (τ) depended strongly on wavelength detection (λ) [6–9]: τ decreases with decreasing λ. For example τ is 45 μs at 700 nm and 5 μs at 550 nm [9]. M'ghaïeth et al. [4] have studied the TRPL of fresh and oxidized PS at different time delay. They reported that the PL peak energy position of oxidized PS shifted to high wavelength unlike of that fresh PS where its PL peak is maintained at the same position. This behavior was attributed to the dependence of the decay rate of the wavelength in the oxidized PS.

However, a major drawback of PS is the inefficacity and the instability [10,11] of its optical characteristics. To resolve these inconvenient, Chen et al. [12] have passivated the silicon dangling bonds of PS by iron using hydrothermal erosion technique. The contamination of PS by Fe induces an increase of PL intensity and after 4 months subsequent to preparation the PL is stabilised. We [13] have showed that iron in PS pores quenched the silicon dangling bonds and consequently the PL intensity increases without any change of the PL band energy during the exposition of iron–PS sample to ambient air as it has been reported by Lee et al. [14]. These results are due to the protection of Si nanocrystallites (nc-Si) by iron.

To our knowledge, the TRPL of stabilised PS structure by iron (PS/Fe) has not been studied and the electron–hole recombination paths in PS/Fe nanocomposites are not well understood.

In this work, we study the effect of electronic iron levels in the enhancement of radiative recombination process using TRPL measurements of PS/Fe sample with delay time, after the end of laser pulse, ranging from 0 μs up to 75 μs at room temperature. The decay curves at the principal band energies are also studied. The TRPL measurements, at different delays, and the analyses of the decay time helped us to establish the role of iron in the luminescence process of PS/Fe nanocomposites.

2. Experimental

The PS is prepared by electrochemical anodisation of boron-doped p-type (100)-Si substrate, with 1–4 Ω cm resistivity. The back side of the wafer was coated with Al and then annealed at 500 °C for 30 min. The electrolyte was composed of a solution of HF (40%)/C_2H_5OH/H_2O (2:1:1), the current density was fixed at 10 mA/cm^2

* Corresponding author at: Unité de Spectroscopie Raman, Faculté des Sciences de Tunis, Université Tunis El Manar, 2092 ElManar, Tunis, Tunisia.
E-mail address: MohamedAli.zaibi@fsb.rnu.tn (M.-A. Zaïbi).

0925-8388/$ – see front matter © 2010 Elsevier B.V. All rights reserved.
doi:10.1016/j.jallcom.2010.07.055

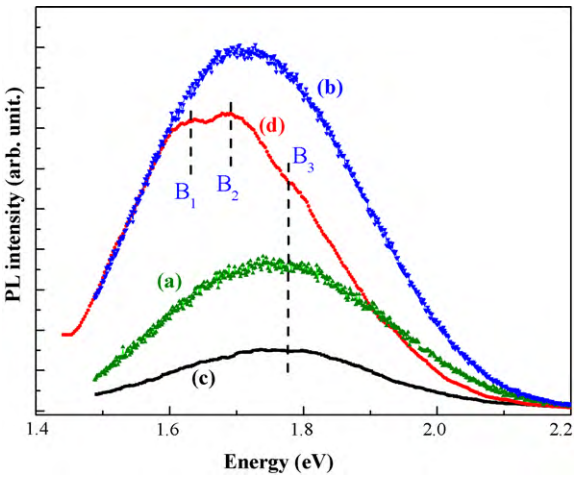

Fig. 1. TRPL spectra compared to CW-PL of PS and PS/Fe samples: PL of PS (a), PS/Fe (b) and TRPL of PS (c), PS/Fe (d).

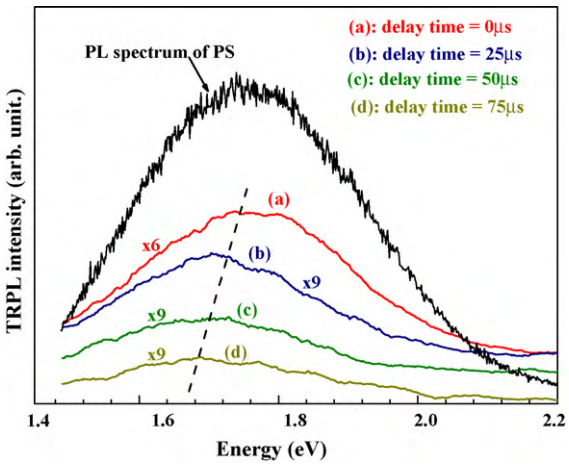

Fig. 2. TRPL spectra of PS at different delays (0, 25, 50 and 75 μs) after the end of laser pulse and PL spectrum. TRPL spectra have been amplified to be compared with the PL spectra.

and the etching time was equal to 10 min. PS/Fe was prepared by impregnation of PS layer, during 5 min, in 0.3 M ferric nitrate aqueous solution, maintained at room temperature. To eliminate the residual gases, the samples were been dried by nitrogen gas.

A triple monochromator and a GaAs photomultiplier were used to record the PL and TRPL spectra. The samples were excited by 488 nm line of an Ar^+ laser.

The PL decays as well as the time-delayed PL spectra were obtained by a time correlated photon-counting technique. The samples were excited by the pulses of an acousto-optic cell (repetition rate: 2 MHz; pulse width 100 μs). Time decays were round up by a gated-photon counter with a temporal resolution of 5 ns.

3. Results and discussion

Fig. 1 presents the TRPL and CW-PL spectra of PS and PS/Fe samples recorded at room temperature. The TRPL spectra are recorded just after the end of the laser pulse. The principal modifications in PL and TRPL of PS/Fe spectra to PS are: (i) the enhancement of PL intensity of the overall spectrum, (ii) the apparition of new bands centred at 1.63 eV (B_1), 1.69 eV (B_2) and 1.77 eV (B_3). The band B_3 on TRPL spectrum of PS/Fe is, also, shown in TRPL spectrum of PS. B_3 corresponds, necessarily, to the band gap energy distribution of porous silicon.

The passivation of PS by iron may modify the recombination kinetics since it introduces new radiative recombination paths, which enhances the photoluminescence intensity.

The time-delayed PL spectra of PS at room temperature recorded at 0, 25, 50 and 75 μs after the end of the laser pulse, using a temporal acquisition window of 25 μs, are shown in Fig. 2. The PL spectrum of PS under continuous excitation is also reported in the same figure. The luminescence intensity decreases rapidly with increasing the time delay. However, the TRPL spectrum associated to the first delay time 0 μs has practically the same shape and is centred at the same energy than the PL one. For the other delayed times, the TRPL spectrum has a red shift from 1.77 to 1.70 eV.

Using the same measurement conditions of PS sample (time-delayed, temporal window, power excitation), the time-resolved experiments of PS/Fe were carried out. The time-delayed spectra as well as PL spectrum of PS/Fe are presented in Fig. 3. The intensity of the time-delayed PL spectrum decreases as the delay time increases but less than in the PS.

It is well known that the radiative recombination of excited carriers, inside the PS layer, involves different size of crystallites. The PL or TRPL can be decomposed as a sum of multi-Gaussian, depending on the sample preparation conditions. The temporal evolution of the PL shape is attributed to the change of the full-width at half maximum (FWHM) of multi-Gaussian rather than the shift of the band gap. Fig. 4 shows the evolution of multi-Gaussian fit of selected TRPL from Fig. 2 (delayed time 0, 50 and 75 μs). The Gaussian amplitude corresponding to blue energy (small crystallites) decreases with increasing the time delay faster than the Gaussian amplitude of the red energy (large crystallites). The same results are reported by Lukasiak et al. [5].

The deconvolution of each TRPL of PS/Fe (for delayed time 0, 50 and 75 μs) as a sum of multi-Gaussian centred at B_1, B_2 and B_3 is shown in Fig. 5. The important contribution to each TRPL spectrum is due to nc-Si at 1.69 and 1.63 eV but the contribution of the nc-Si at 1.77 eV is less important when the delayed time increases. From this result, we can highlight that the PL of PS/Fe is due, largely, to the radiative transitions of nc-Si at 1.69 and 1.63 eV.

At the same energy of 1.77 eV, we have plotted in Fig. 6, the TRPL of PS and PS/Fe versus time. Then each curve has been fitted by the well-known stretched exponential [10]:

$$I(t) = I_0 \exp\left(-\frac{t}{\tau}\right)^{\beta} \quad \text{(i)}$$

where $I(t)$ and I_0 are the PL intensities at time t and 0, respectively, τ reflects both the radiative (τ_R) and the non-radiative (τ_{NR}) recombination time. The dispersion factor β ($0 \le \beta \le 1$) arises from communication between nanocrystals during the recombination processes. The adequate fits are shown as solid curves in Fig. 6, illustrating a good agreement of the fits and which provides value

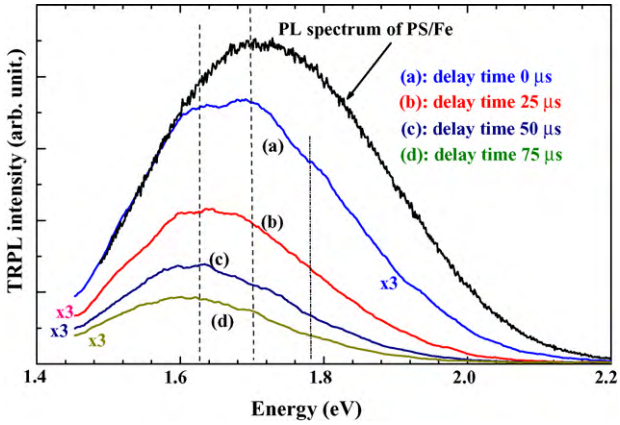

Fig. 3. TRPL spectra of PS/Fe at different delays (0, 25, 50 and 75 μs) after the end of laser pulse and PL spectrum. TRPL spectra have been amplified to be compared with the PL spectra.

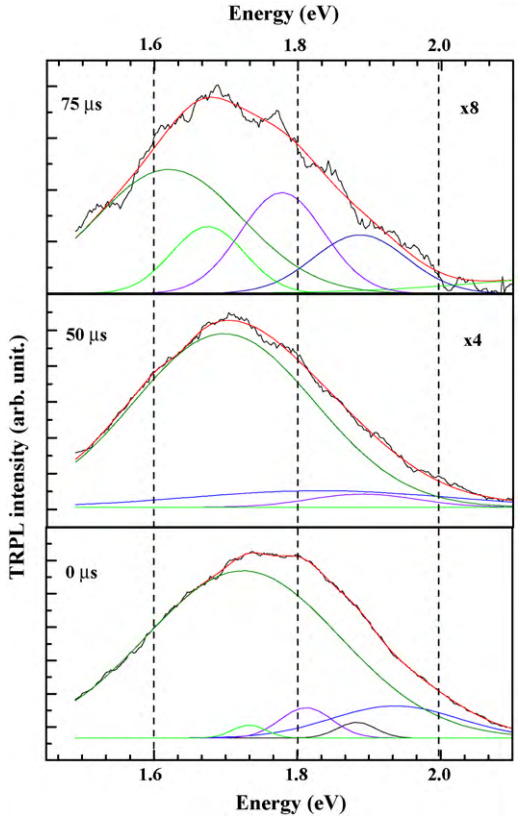

Fig. 4. Examples of multi-Gaussian fit of selected TRPL spectra from Fig. 2. TRPL spectra have been amplified to be compared with the TRPL spectrum at 0 µs.

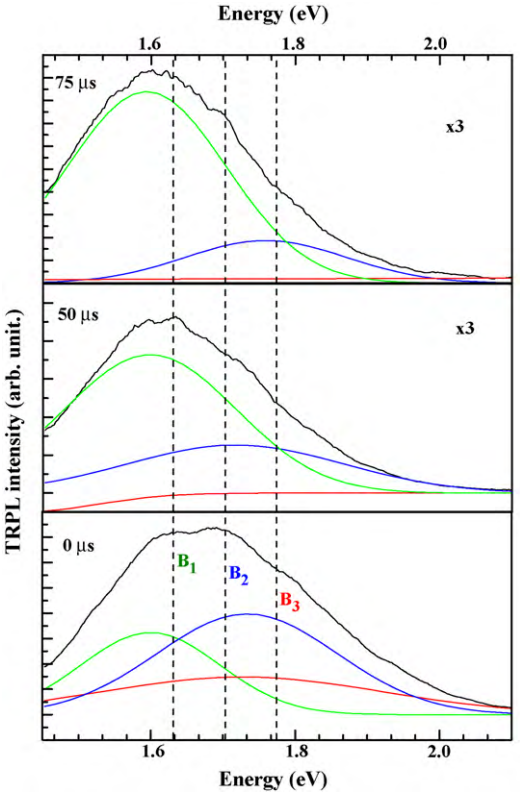

Fig. 5. Examples of multi-Gaussian fit of PS/Fe TRPL spectra. TRPL spectra have been amplified to be compared with the TRPL spectrum at 0 µs.

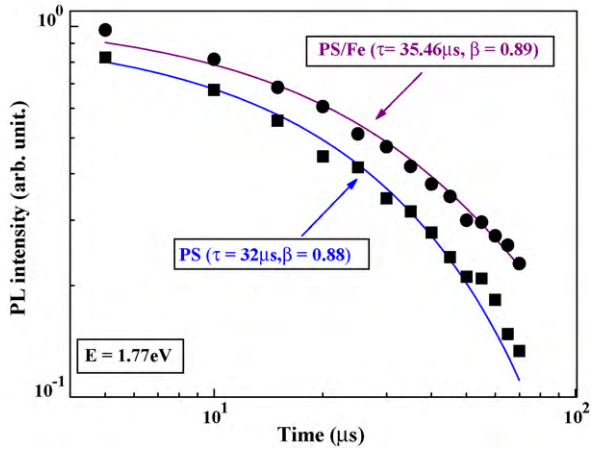

Fig. 6. Photoluminescence decay profiles of PS and PS/Fe samples at 1.77 eV.

of the fitting parameters τ and β (see Fig. 6). The β parameter does not present a significant variation, and then we can consider that the dispersion factor is the same for PS and PS/Fe. While the decay time (τ) is larger in PS/Fe then in PS. The introduction of Fe in PS pores leads to the formation of new radiative recombination paths, attributed to B_1 and B_2, and than an increase of τ; τ (PS/Fe) superior to τ (PS). This increase of τ is necessarily due to reduced non-radiative paths. Lukasiak et al. [5] reported that non-radiative recombination occurs when excited carriers escape by tunnelling from small crystallites to larger ones or less passivated region of nc-Si. Also, the average decay time τ increases when the radiative process dominates over slower non-radiative process. The incorporation of iron in PS passivated the nc-Si then reduces the non-radiative process, which becomes more and more dominated by radiative recombination and consequently an increasing of the average decay time τ. The elimination of PS non-radiative paths was also reported by Chen et al. [15] in the case of PS covered by MnO_2 layer using hydrothermal technique. MnO_2 induces a high potential barrier which prevents excited carrier diffusion from the core nc-Si to neighbouring defects from non-radiative recombination. Then, we conclude that the passivation of PS by iron introduces new transitions and simultaneously reduces the non-radiative recombination.

In addition to B_3, the fit of TRPL of B_1, B_2 by $I(t)$, with β equal to 0.89, gives a decay time which was increased from B_1 to B_3 (Fig. 7). Such variation is in concordance with experimental [4,9]

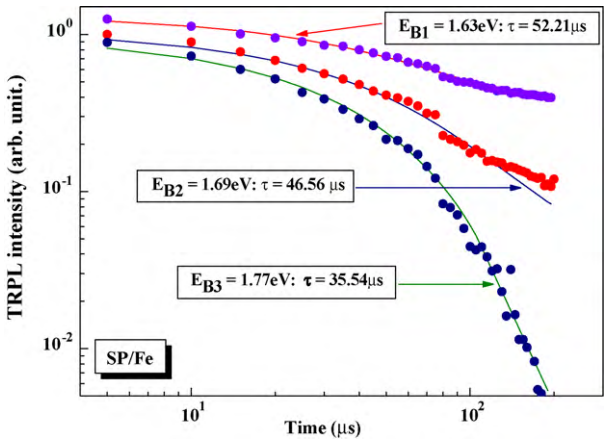

Fig. 7. Decay curves of TRPL from PS/Fe sample corresponding to 1.63, 1.69 and 1.77 eV.

Table 1
The variation of α parameter with delayed time.

Delay time (μs)	0	25	50	75
$\alpha = J(B_2 = 1.69\,eV)/J(B_1 = 1.63\,eV)$	1.33	1.13	0.34	0.29

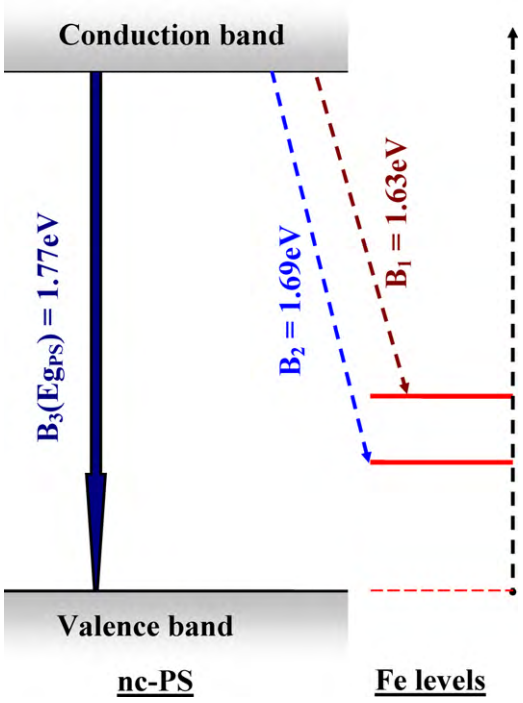

Fig. 8. Proposed schematic recombination paths in PS/Fe nanocomposites; highlighting the two iron energy levels located in the PS band gap.

and numerical [16] analysis which they have found that the PL decay time decreases when the emission energies increase.

Yang et al. [17] have investigated the TRPL of aluminium oxide, and have observed a decrease of the decay time with increasing the emission energy. This evolution has been explained by the carriers' localization effect characterized by the radiative recombination. Such effect is due to the localized sites introduced by surface states or structural disorder. This result is in concordance with that found in our case and agrees with the localized states generated by iron in the PS gap.

To have an idea of the contribution of B_1 and B_2 during the delayed time, we examined the ratio of their relative integrated intensity (J); α is this ratio: $\alpha = J(B_2 = 1.69\,eV)/J(B_1 = 1.63\,eV)$. The calculated values of α are presented in Table 1. The evolution of α suggests that the radiative transitions at 1.63 eV decreases very slowly with delayed time than at 1.69 eV.

All these results indicate that the passivation of PS by iron introduces levels in the PS band gap and reduces non-radiative recombination of the nc-Si. The conjugation of our previous results [13,18] and this work shows that the recombination kinetics in PS/Fe is doing through two levels localized in the PS band gap. Consequently, we attribute B_1 and B_2 to levels in the band gap of PS. Fig. 8 presents a schematic energy diagram of PS/Fe. It is not the first one where the iron introduces levels in the gap; the same result has been reported by Dŏgan et al. [19] when they have incorporated the same metal (iron) in InP at 300 K.

4. Conclusion

We have studied time-resolved photoluminescence spectra of porous silicon and stable porous silicon/iron nanocomposites at room temperature for different delay times. The presence of iron in porous silicon matrix induces two energy levels localised in the PS band gap. Such levels modify the recombination processes by creating new radiative recombination paths and reduce the non-radiative transition. The disappearance of non-radiative recombination confirms the passivation of nc-Si by iron.

References

[1] L.T. Canham, Appl. Phys. Lett. 57 (1990) 1046.
[2] J. Kudrna, P. Bartosek, F. Trojanek, I. Pelant, P. Maly, J. Lumin. 72–74 (1997) 347.
[3] J.C. Vial, A. Bsiesy, F. Gaspard, R. Herino, M. Ligeon, F. Muller, R. Romestain, Phys. Rev. B 45 (1992) 14171.
[4] R. M'ghaïeth, H. Maâref, I. Mihalcescu, J.C. Vial, Microelectron. J. 30 (1999) 695.
[5] Z. Lukasiak, P. Dalasinski, W. Bala, Opto-electron. Rev. 11 (2003) 113.
[6] G.W. t'Hooft, Y.A.R.R. Kessener, G.L.J.A. Rikken, A.H.J. Venhuizen, Appl. Phys. Lett. 61 (1992) 2344.
[7] X. Chen, B. Henderson, K.P. O'Donnell, Appl. Phys. Lett. 60 (1992) 2672.
[8] N. Ookubo, H. Ono, Y. Ochiai, Y. Mochizuki, S. Matsui, Appl. Phys. Lett. 61 (1992) 940.
[9] A. Bsiesy, J.C. Vial, F. Gaspard, R. Herino, M. Ligeon, F. Muller, R. Romestain, A. Wasiela, A. Halimaoui, G. Bomchil, Surf. Sci. 254 (1991) 195.
[10] O. Bisi, S. Ossicini, L. Pavesi, Surf. Sci. Rep. 38 (2000) 1.
[11] A.G. Cullis, L.T. Canham, P.D.J. Calcott, J. Appl. Phys. 82 (1997) 909.
[12] Q.W. Chen, X. Li, Y. Zhang, Chem. Phys. Lett. 343 (2001) 507.
[13] M. Rahmani, A. Moadhen, M.-A. Zaïbi, H. Elhouichet, M. Oueslati, J. Lumin. 128 (2008) 1763.
[14] D.Y. Lee, J.W. Park, J.Y. Leem, J.S. Kim, S.K. Kang, J.S. Son, H.B. Kang, Y.H. Mun, D.K. Lee, D.H. Kim, I.H. Bae, J. Cryst. Growth 260 (2004) 394.
[15] Q. Chen, Y. Zhang, Y.T. Qian, J. Phys. Condens. Matter 13 (2001) 5377.
[16] R. Laiho, A. Pavlov, T. Tsuboi, J. Lumin. 57 (1993) 89.
[17] M.D. Yang, K.W. Chen, J.L. Shen, J.C. Wang, C. Hsu, Nanotechnology 18 (2007) 405707.
[18] M. Rahmani, A. Moadhen, M.-A. Zaïbi, A. Lusson, H. Elhouichet, M. Oueslati, J. Alloys Compd. 485 (2009) 422.
[19] S. Doğan, S. Tüzemen, J. Lumin. 128 (2008) 232.